ON TIME-INTERLEAVED ANALOG-TO-DIGITAL CONVERTER FOR WIDEBAND RECONFIGURABLE RADIOS

Michael Soudan (Institute of Microelectronics and Wireless Systems: National University of Ireland, Maynooth, Kildare, Ireland; msoudan@eeng.nuim.ie);
Ronan Farrell (Institute of Microelectronics and Wireless Systems: National University of Ireland, Maynooth, Kildare, Ireland; rfarrell@eeng.nuim.ie);

ABSTRACT

This paper presents a transceiver model that comprises two time-interleaved analog-to-digital converter (ADC) systems to sample the inphase and quadrature signals in a digital receiver. Random data is used as the information signal and quadrature amplitude modulation (QAM) is employed as the modulation scheme. To overcome the performance degradation induced by converter mismatch, two different reconstruction techniques are proposed. An analytical Discrete Fourier Transform description of the non-ideal sampling process is presented to design reconstruction filters that mitigate distortions, caused by non-ideal sampling. Moreover, a novel design technique is presented that allows for the design of reconstruction filters in the time domain. This design methodology proves to be less involved and more concise compared with the frequency based approach. Furthermore, simulation results are presented illustrating the severe degradation of the receiver performance due to moderate converter mismatch for 16 and 64 QAM when no reconstruction filters are employed. Finally, it is shown how the decreased symbol error rate (SER) can be significantly improved by utilizing the proposed reconstruction filters.

1. INTRODUCTION

A common strategy for designing software defined radios is the use of wideband ADCs for capturing large segments of the input spectrum. This enables the subsequent digital signal processing blocks to select channels, extract the information signals and provides versatile functionality to the receiver [1]. This fuels the demand of ADCs with high sampling rates, providing sufficient resolution for the given application. In narrowband system where automatic gain control and analogue channel select filters can be used, suitable dynamic range can be assumed to be available at the ADCs. However, for captured wideband spectra, the required resolution of these ADCs is determined by the necessity to detect weak information signals while strong blocking signals cover the full input range of the converter. For example, the GSM standard requires a sensitivity of -102 dBm in the presence of a 0 dBm blocking signal which amounts to 102 dB of spurious free dynamic range. As a consequence, high resolution converters (15-16 bit) are required to capture the information signal [2].

To meet the ever increasing demand of wideband converters, the usage of multiple ADCs in a time-interleaved manner has been proposed [3]. This architecture combines several ADCs, called channels, into a single effective ADC by interleaving the input sampling times of the channel ADCs [4]. This approach allows the use of power efficient and inexpensive channel ADCs that are many times slower than the overall sampling rate. Utilising time-interleaving techniques with a large number of channel ADCs theoretically facilitates an substantial enhancement of the overall sampling rate, preserving a high dynamic range and doing so in a power efficient manner. Equally, the bandwidth or power consumption of the system is easily adjusted by changing the number of channel ADCs being used. Unfortunately, mismatches between the individual ADC characteristics cause spurious images in the output spectrum. In particular, gain, offset and timing mismatch create spurious images in the output spectrum. Even small timing mismatch severely degrades the spurious free dynamic range and the signal-to-noise ratio of the output signal and better than 10 bit of performance is difficult to achieve.

This performance penalty can be overcome by modeling the individual channel characteristics by finite impulse response (FIR) fractional filters, and thereby constructing a mismatch affected sampling system [5]. In this paper, a frequency and a time-based description of such a system are derived for reconstructing the original from the distorted data. In the frequency domain, analytical equations based on the Discrete Fourier Transform (DFT) are employed to describe the distortion mechanisms. Moreover, an alternative novel time-based criterion is presented, whose description of the non-ideal distortions is facilitated in a less involved and more concise manner compared with the frequency based approach. For both the time and frequency based techniques distortion functions are given that allow for the design of reconstruction filters that mitigate the induced distortions in the output spectrum. The proposed reconstruction scheme is utilized in a direct conversion architecture where non-ideal

time-interleaved converters are used in the inphase and quadrature branches.

Eventually, simulations demonstrate the SER degradation for 4, 16 and 64 QAM schemes that can be expected due to converter mismatch. The results indicate that even for the most challenging modulation scheme (64 QAM) and a low synthesis filter order of 8, the SER of the reconstructed data matches at least to 96 percent the expected SER for various energy per bit ratios of 11 to 20 dB.

2. TIME-INTERLEAVED A/D CONVERTER

For ADCs that operate in a time-interleaved manner, the overall sampling rate f_s becomes a multiple of the sampling rate of a single ADC f_{AD}, according to the number of employed ADCs M. The sampling instants t_m of the individual converters, called channels, are controlled by their dedicated clock signals, where $m = [0, 1, .., L]$ indicates the channel index. The digital output of the different channels is serialized in the last stage (see Fig. 1)

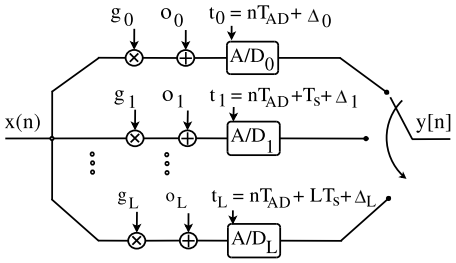

Fig. 1. Time-interleaved system employing non-ideal converters in a time-interleaved manner.

3. QAM TRANSCEIVER MODEL

Fig. 2 depicts an idealised direct conversion architecture which was choosen for its ability to tune across a wide selection of channel bandwidths and its application in current SDR prototypes, such as the Maynooth Adaptable Radio System (MARS). The transceiver model utilises quadrature QAM and matched filtering to minimize the impact of white Gaussian noise that affects the transmission channel [6].

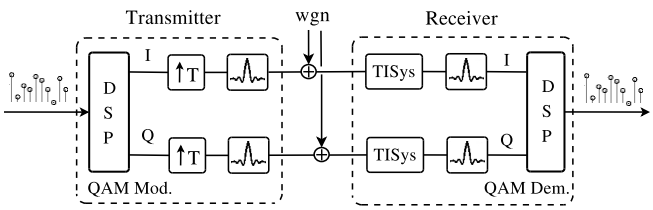

Fig. 2. QAM Transceiver model utilizing time-interleaved converter systems in both I and Q branch.

QAM modulation was selected as the modulation scheme due to its widespread use in current and emerging technologies and low susceptibility to channel noise. To account for realistic input data, a uniformly distributed random signal is used as an input for the transmitter. On the receiver side, both I and Q signals are sampled by two dedicated time-interleaved ADC systems (see Section 2). For the I channel, different Gaussian distributions with various standard deviations are used to characterise the gain, offset and timing mismatch errors. The mean values of all distribution are assumed to be zero. Three sets of identical but independent distributions are employed to describe the corresponding Q channel mismatch errors, since two separate conversion systems are utilized in the transceiver model. The converted I and Q signals are then filtered by the matched filters of the receiver and demodulated in the last stage.

4. DISTORTION CANCELLATION

The two presented design methods are based on the description of the non-ideal sampling process in the frequency and time domain, respectively. For both techniques, distortion functions are derived that describe how the input data and higher frequent undesired images are shaped. By specifying the desired distortion coefficients, the respective system of equations can be solved for synthesis filter that do not distort the desired signal but suppress its spurious images.

4.1. Reconstruction in the Frequency Domain

Filter bank theory can be used to model the behaviour of time-interleaved converter systems (see Fig. 3). Each time-interleaved ADC is described as a channel of the maximally decimated filter bank. A channel dependant delay followed by a decimation stage models the recurrent sampling of a single converter at a lower sampling rate. The converters non-ideal behaviour, constituted by gain, offset and timing mismatch errors, is described by an pre-processing analysis filter H_m, where m indicates the channel index.

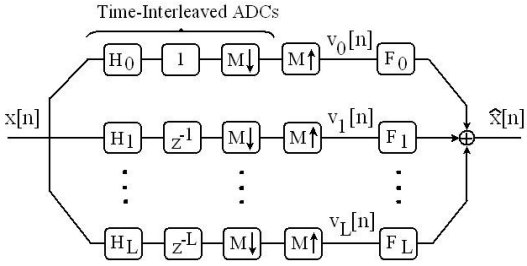

Fig. 3. M channel filter bank modeling a non-ideal converter system operating in a time-interleaved manner.

The downsampled distorted data is upsampled and the resulting signal $v_m[n]$ is processed by the synthesis filter F_m. In the case no reconstruction is desired, the synthesis filters introduce only a channel dependent delay to demultiplex the individual converter data to a single output stream.
The spectrum of the distorted channel data is given in (1) [7], where the discrete angular frequency Ω_k equals $2\pi k/N$ and N indicates the number of frequency bins. The overall filter bank output is the superposition of all upsampled channel data filtered by its corresponding synthesis filter (2) [7].

$$V_m(e^{j\Omega_k}) = \frac{1}{M}\sum_{l=0}^{M-1} H_{lm}(e^{j\Omega_k}) X(e^{j(\Omega_k-\Omega_l)}) \quad (1)$$

$$\hat{X}(e^{j\Omega_k}) = \frac{1}{M}\sum_{m=0}^{M-1} V_m(e^{j\Omega_k}) F_m(e^{j\Omega_k}) \quad (2)$$

The spectrum of the output signal can now be rewritten in terms of distortion coefficients which shape the original input spectrum as well as the undesired images located at integer multiples of $2\pi/M$ on the frequency axis .

$$\hat{X}(e^{j\Omega_k}) = \frac{1}{M}\sum_{l=0}^{M-1} A_l(e^{j\Omega_k}) X(e^{j(\Omega_k-\Omega_l)}) \quad (3)$$

$$A_l(e^{j\Omega_k}) = \frac{1}{M}\sum_{m=0}^{M-1} H_{lm}(e^{j\Omega_k}) F_m(e^{j\Omega_k}) \quad (4)$$

The distortion coefficients given in (4) can be expressed in a matrix form [7], where the elements of matrix H are determined by the frequency translated spectra of the analysis filter (5).

$$\underbrace{\begin{bmatrix} A_0(e^{j\Omega_k}) \\ A_1(e^{j\Omega_k}) \\ \vdots \\ A_L(e^{j\Omega_k}) \end{bmatrix}}_{A(e^{j\Omega_k})} = \frac{1}{M} \underbrace{\begin{bmatrix} H_{00}(e^{j\Omega_k}) & \cdots & H_{L0}(e^{j\Omega_k}) \\ H_{01}(e^{j\Omega_k}) & \cdots & H_{L1}(e^{j\Omega_k}) \\ \vdots & \ddots & \vdots \\ H_{0L}(e^{j\Omega_k}) & \cdots & H_{LL}(e^{j\Omega_k}) \end{bmatrix}}_{H(e^{j\Omega_k})} \underbrace{\begin{bmatrix} F_0(e^{j\Omega_k}) \\ F_1(e^{j\Omega_k}) \\ \vdots \\ F_L(e^{j\Omega_k}) \end{bmatrix}}_{F(e^{j\Omega_k})} \quad (5)$$

To model the non-ideal behaviour of the samplers, the timing mismatch of each channel is represented as the spectrum of a channel dependent fractional delay (see (6) and (7)).

$$H_m(e^{j\Omega_s}) = e^{-j\Omega_s d_m} \quad (6)$$

$$d_m = \frac{N}{2} - 1 - \Delta_m + m \quad (7)$$

The resulting description of the frequency translated spectrum of the analysis filter is rather involved since the higher frequent spectra show a nonlinear phase response (see Appendix 7.2) as has been pointed out by the authors of [8] for the 2 channel case. (8) gives the general description of spectra for an arbitrary number of channels.

$$H_{lm}(e^{j\Omega_s}) = \left[\Pi_l(e^{j\Omega_s})\left(e^{-j2\pi\, d_m} - 1\right) + 1\right] e^{-j(\Omega_s - 2\pi\frac{l}{M})d_m} \quad (8)$$

The window function is given in (9) for M being a integer multiple of N.

$$\Pi_l = \begin{cases} 1 & for \quad \Omega_s \le -\pi\left(1 - l\ 2/M + 2/N\right) \\ 0 & for \quad \Omega_s > -\pi\left(1 - l\ 2/M + 2/N\right) \end{cases} \quad (9)$$

(3) shows that to obtain perfect reconstruction, the distortion coefficient $A_0(e^{j\Omega k})$ is has to be an ideal bandpass whereas all other coefficients are ideal bandstop filters.
With these descriptions of H and A, the set of reconstruction filter F can be obtained by solving the system of equations given in (5), i.e.

$$F(e^{j\Omega_k}) = M\ \left(H(e^{j\Omega_k})\right)^{-1}\ A(e^{j\Omega_k}) \quad (10)$$

4.2. Reconstruction in the Time Domain

The distorted upsampled data can be described as the summation of the impulse responses h_{lm} convolved with the modulated signal $x[n]$, where $n = [0, 1, \ldots, N-1]$.

$$u_m[n] = \frac{1}{M}\sum_{l=0}^{M-1} h_{lm}[n - N/2 + 1] \otimes \left(x[n]\ e^{j2\pi\frac{l}{M}n} \right) \quad (11)$$

The reconstructed system output is given in (12), where D indicates the delay introduced by the convolution with the synthesis filter.

$$\hat{x}[n - D] = \sum_{m=0}^{M-1} u_m[n]\ \otimes f_m[n] \quad (12)$$

(12) can be rewritten in terms of its distortion coefficients, i.e.

$$\hat{x}[n - D] = \sum_{l=0}^{M-1} a_l[n]\ \otimes \left(x[n]\ e^{j2\pi\frac{l}{M}n} \right) \quad (13)$$

$$a_l[n] = \frac{1}{M}\sum_{m=0}^{M-1} h_{lm}[n] \otimes f_m[n] \quad (14)$$

The sampling system that represents these equations is shown in Fig. 4.

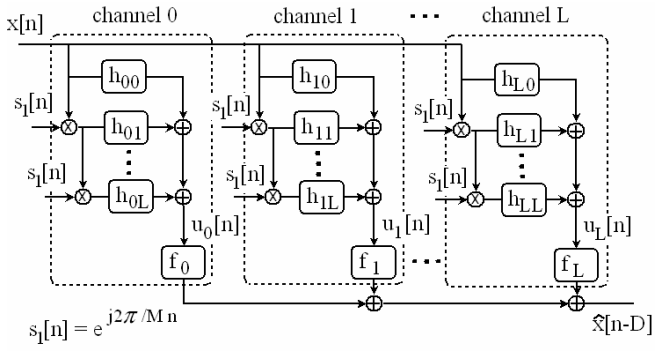

Fig. 4. Time domain representation of a M channel time-interleaved converter.

Similar to the reconstruction criteria in the frequency domain, a system of equations can be defined (see (15)).

$$\underbrace{\begin{bmatrix} a_0[n] \\ a_1[n] \\ \vdots \\ a_L[n] \end{bmatrix}}_{a} = \frac{1}{M} \underbrace{\begin{bmatrix} h_{00}[n] & \cdots & h_{L0}[n] \\ h_{01}[n] & \cdots & h_{L1}[n] \\ \vdots & \ddots & \vdots \\ h_{0L}[n] & \cdots & h_{LL}[n] \end{bmatrix}}_{h} \underbrace{\begin{bmatrix} f_0[n] \\ f_1[n] \\ \vdots \\ f_L[n] \end{bmatrix}}_{f} \tag{15}$$

To obtain the elements of matrix h, the impulse response of the frequency shifted spectrum of an arbitrary analysis filter can be expressed in terms of the original impulse response as shown in (16) (see Appendix). The shift of the modulation index *n* by *m* models the individual sampling instants of each channel. This equation is valid for any system, where the group delay of the analysis filter increases according to its channel index.

$$h_{lm}[n] = h_{0m}[n]\ e^{j2\pi \frac{l}{M}(n-m)} \tag{16}$$

The integer group delay of all analysis filters is not channel dependent and therefore equal when the fractional part is not taken into account as shown in (17).

$$r_m = \frac{N}{2} - 1 - \Delta_m \tag{17}$$

The causal complex impulse response of an ideal frequency shifted analysis filter is given (see Appendix 7.1), i.e.

$$h_{lm}[n] = \frac{e^{j\pi(r_m - n)} - e^{-j\pi(r_m - n)}}{N - N\ e^{-j2\pi(r_m - n)}}\ e^{j2\pi \frac{l}{M}(n-m)} \tag{18}$$

The distortion function *a0* is given by the dirac delta function *δ[n]* for *n=[0, 1, …, N-1]*, whereas all other distortion functions are zero for all *n*. The set of reconstruction filters can be derived by (19).

$$f = M\ (h)^{-1}\ a \tag{19}$$

5. SIMULATIONS

5.1. Reconstruction in the Time Domain Using Complex Impulse Responses

To verify the time-based reconstruction technique, a non-uniformly sampled three-tone signal was applied to a four channel filter bank with the channel delays Δ= [0.05, -0.13, -0.3, 0.45]. The elements of matrix H were calculated using the complex impulse responses given in (18). The frequencies of the sinusoidal components were chosen to be high fractional frequencies which is typically challenging for reconstruction filters (f_0=240/1024 f_s, f_1=320/1024 f_s and f_2= 496/1024 f_s). Fig. 5 shows accuracy of the analysis and synthesis filtering part of the system, separately. In Fig. a) a uniformly sampled signal is processed by the analysis part of the system only and no reconstruction is employed. The very high SNR of 283 dB indicates that the analysis part of the system models the nonuniform sampling processes with a very high accuracy. To observe the performance of the synthesis part of the system only, a nonuniformly sampled signal is downsampled and upsampled using a channel dependent sampling phase. The respective channel data is filtered with the corresponding channel synthesis filter and all channel outputs are added. The filterbank output is compared with the ideal uniform signal and a SNR of 276 dB is obtained.

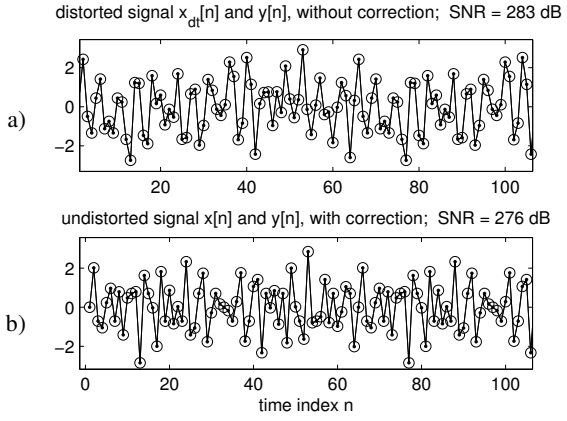

Fig. 5. SNR performance of (a) analysis and (b) synthesis part of reconstruction scheme.

5.2. Reconstruction in the Time Domain of I/Q Receiver Data

The model presented in Section 3 has been simulated using 1000 uniformly distributed data points as an input sequence for the quadrature amplitude modulator. In this section, the presented figures-of-merit such as SER and signal-to-noise ratio (SNR) show the average value of at least 500 simulations to provide results of sufficient statistical significance. The specified standard deviations g and Δ were used to select the respective mismatch magnitudes of the individual converters for every simulation. Using these mismatch values, the analysis filter were designed as Hann windowed sinc filters of order 8. The obtained impulse responses of synthesis filter were real valued and of the same order as the analysis filer. The modulation and demodulation of the information signal and the transmitter matched filter design were carried out in Matlab. The roll-off and oversampling factor and the filter delay were selected to be *[0.2, 2, 16]* for the matched filter design, respectively.

Its finite length of 65 taps introduced an mean-squared-error of 54.8 dB for a random 64 QAM signal, when no other noise source affected the transceiver. 14-bit ADCs were employed in the time-interleaved system, unless stated otherwise. Matched root-raised-cosine filtering was performed at the filterbank output to mitigate the impact of white Gaussian channel noise.

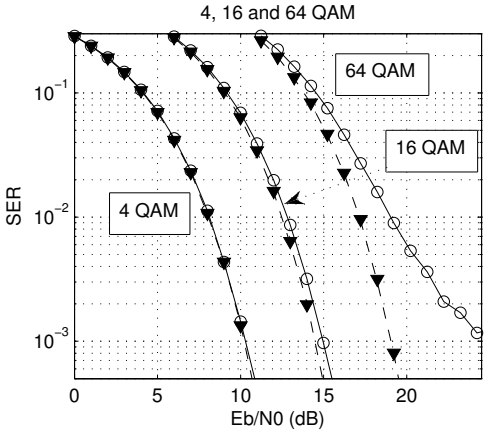

Fig. 6. Symbol error rate against Eb/N0 for 4, 16 and 64 QAM with (solid lines with circular markers) and without mismatch errors (dashed lines). The SER of the reconstructed signal is indicated by triangles. ([g; Δ] = [5%; 5%]).

Fig. 6 shows the symbol error rate against the energy per bit to noise power spectral density ratio E_b/N_0 for 4, 16 and 64 QAM. The dashed lines indicate the symbol error performance, when the ADCs do sampling related errors due to channel mismatch. The solid lines show the additional impact of gain, offset and timing mismatch error on the SER. The standard deviations of gain and timing mismatch error were selected to be 5% each.

As depicted in this figure, the 4 QAM system is hardly affected by the mismatch errors due to the great Euclidean distance of its constellation points. However, an increasing number of constellation points in combination with the specified mismatch errors increases the symbol error rate of the 16 and 64 QAM modulation system significantly. To reduce this performance penalty, reconstruction filter were designed with an order of 8. The SER of the reconstructed data is indicated by triangles for all QAM schemes.

6. CONCLUSION

The impact of ADC non-idealities such as gain and timing mismatch on the digital receiver performance was investigated. The figures-of-merit degradation that can be expected for moderate converter mismatch has been demonstrated for different quadrature amplitude modulation schemes. Simulation results indicate that A/D mismatch severely increases the receiver symbol error rate for higher order QAM systems. To overcome these performance penalties, a time and a frequency domain based correction scheme was derived to design reconstruction filters. Employing these reconstruction filters, the symbol error rate was enhanced significantly close to the ideal value.

7. REFERENCES

[1] J. Mitola, “Software radios: Survey, critical evaluation and future directions”, *IEEE Aerospace and Electronic Systems Magazine*, vol. 8, pp. 25-36, 1993.

[2] GSM Standard, 3GPP (3rd Generation Partnership Project), http://www.3gpp.org.

[3] T. Tsai, P. J. Hurst, S. H. Lewis, "Time-Interleaved Analog-to-Digital Converters for Digital Communications," *Conf. on Circuits, Signals and Systems*, pp. 193-198, 2004.

[4] W. Black, D. Hodges, “Time interleaved converter arrays,” *IEEE J. Solid-State Circuits*, vol. SC-15, pp. 1022-1029, 1980.

[5] R. Prendergast, “Reconstruction of Band-Limited Periodic Nonuniformly Sampled Signals Through Multirate Filter Banks”, *IEEE Trans. on Circuits and Systems*, vol. 51, pp. 1612-1622, 2004.

[6] J. Proakis, "Digital Communications", McGraw-Hill, Inc., New York, 10020, third edition, 1995.

[7] P. P. Vaidyanathan, Multirate Systems and Filter Banks, Englewood Cliffs, NJ: Prentice-Hall, 1993.

[8] P. Sommen, K. Janse, „On the relationship between uniform and recurrent nonuniform discrete-time sampling schemes“, *IEEE Transactions on Signal Processing*, vol. 56, no. 10, pp. 5147-5156, 2008.

8. APPENDIX

8.1. Frequency Translated Impulse Response of the Analysis Filter

The spectrum of an ideal allpass that introduces a fractional delay can be described by the DFT, i.e.

$$H_m\left(e^{j\Omega_k}\right) = e^{-j\Omega_k d_m} \tag{20}$$

The impulse response of this allpass filter can be derived by applying the IDFT

$$h_m[n] = \frac{1}{N}\sum_{k=-N/2}^{N/2-1} e^{-j\Omega_k (d_m - n)} \tag{21}$$

By applying a shifted DFT we obtain the frequency shifted spectrum of the ideal allpass filter

$$H_{lm}\left(e^{j\Omega_p}\right) = \sum_{n=0}^{N-1}\frac{1}{N}\sum_{k=-N/2}^{N/2-1} e^{-j\Omega_k (d_m - n)}\; e^{-j(\Omega_p - 2\pi\frac{l}{M})n} \tag{22}$$

By reordering the terms and solving the inner summation, the impulse response of the frequency translated spectrum can be obtained (see (23) and (25)).

$$H_{lm}\left(e^{j\Omega_p}\right) = \sum_{n=0}^{N-1} h_{lm}[n]\; e^{-j\Omega_p n} \tag{23}$$

$$h_{lm}[n] = \underbrace{\frac{1}{N}\;\frac{e^{j\pi\,(d_m - n)} - e^{-j\pi\,(d_m - n)}}{1 - e^{-j2\pi\,(d_m - n)}}}_{h_{0m}[n]}\; e^{j2\pi\,\frac{l}{M}\,n} \tag{24}$$

(24) is equivalent to (25) that shows the similarity to the Dirchilet kernel.

$$h_{lm}[n] = e^{j\pi\left(\frac{(d_m - n)}{N} + \frac{2l}{M}n\right)}\;\frac{\sin(\pi\;(d_m - n))}{N\sin(\pi\;(d_m - n)/N)} \tag{25}$$

8.2. Frequency Translated Spectrum of the Analysis Filter

From (24) can be seen that the translated impulse response $h_{lm}\,[n]$ is obtained by multiplying $h_{0m}\,[n]$ with the complex signal $s_l\,[n] = exp(\,j\,2\,\pi\,l/M\,n)$ in the time domain. The same result is obtained by convolving the respective spectra in the frequency domain. The spectrum of the modulating signal is given, i.e.

$$S_l\left(e^{j\Omega_k}\right) = \sum_{n=0}^{N-1} e^{-j(\Omega_k - 2\pi\frac{l}{M})\,n} \tag{26}$$

$$S_l\left(e^{j\Omega_k}\right) = \frac{1 - e^{-j(\Omega_k - 2\pi\frac{l}{M})\,N}}{1 - e^{-j(\Omega_k - 2\pi\frac{l}{M})}} \tag{27}$$

The spectrum of the translated frequency spectrum is given in (28)

$$H_{lm}(e^{j\Omega_p}) = \sum_{k=0}^{N-1} H_{0m}(e^{j(\Omega_k - \pi)})\;\; S_l(e^{j(\Omega_p - \Omega_k)}) \tag{28}$$

$$H_{lm}\left(e^{j\Omega_p}\right) = \sum_{k=0}^{N-1} e^{-j(\Omega_k - \pi)d_m}\;\;\frac{1 - e^{-j(\Omega_p - \Omega_k - 2\pi\frac{k+l}{M})\,N}}{1 - e^{-j(\Omega_p - \Omega_k - 2\pi\frac{k+l}{M})}} \tag{29}$$

$$H_{ml}\left(e^{j\Omega_p}\right) = \sum_{k=\frac{l}{M}N}^{N-1+\frac{l}{M}N} e^{-j(\Omega_k - \pi - 2\pi\frac{l}{M})d_m}\;\;\frac{1 - e^{-j(\Omega_p - \Omega_k)\,N}}{1 - e^{-j(\Omega_p - \Omega_k)}} \tag{30}$$

In order to shift the summation index k to 0, the summation in (30) can be split into two summations, i.e.

$$\begin{aligned} H_{lm}\left(e^{j\Omega_p}\right) = &\sum_{k=0}^{N-1} e^{-j(\Omega_k - \pi - 2\pi\frac{l}{M})d_m}\;\;\frac{1 - e^{-j(\Omega_p - \Omega_k)\,N}}{1 - e^{-j(\Omega_p - \Omega_k)}} + \\ &\sum_{k=0}^{\frac{l}{M}N-1}\left(e^{-j2\pi\,d_m} - 1\right) e^{-j(\Omega_k - \pi - 2\pi\frac{l}{M})d_m}\;\;\frac{1 - e^{-j(\Omega_p - \Omega_k)\,N}}{1 - e^{-j(\Omega_p - \Omega_k)}} \end{aligned} \tag{31}$$

Both summations are convolutions of the spectral terms with an ideal allpass filter, whose equation is given in (26) and (27) for l equals 0. By recombining the two summation terms and neglecting the spectral convolution which does not change the result, (32) can be derived.

$$H_{lm}(e^{j\Omega_p}) = \left[\Pi_l(e^{j\Omega_p})\left(e^{-j2\pi\,d_m} - 1\right) + 1\right] e^{-j(\Omega_p - 2\pi\frac{l}{M})d_m} \tag{32}$$